Hydrostatic pressure effect on photoinduced insulator-to-metal transition in the layered organic salt α-(BEDT-TTF)$_2$I$_3$

S. Iwai,[1,2,*] K. Yamamoto,[3] F. Hiramatsu,[1] H. Nakaya,[1] Y. Kawakami,[1] and K. Yakushi[3]
[1]*Department of Physics, Tohoku University, Sendai 980-8578, Japan*
[2]*PRESTO-JST, Kawaguchi 332-0012, Japan*
[3]*Institute of Molecular Science, Okazaki 444-8585, Japan*

(Received 14 September 2007; revised manuscript received 27 November 2007; published 27 March 2008)

The effect of high pressure on the photoinduced insulator-to-metal transition in charge-ordered [bis(ethylenedithio)]tetrathiafulvalene (BEDT-TTF) salt α-(BEDT-TTF)$_2$I$_3$ was investigated using femtosecond spectroscopy under hydrostatic pressure. By applying pressure (P), the lifetime of the initially produced microscopic metallic domain becomes shorter, reflecting that condensation to the semimacroscopic metallic state is disturbed for $P<0.5$ GPa. However, condensation is promoted for $P=0.5-1$ GPa, thereby enhancing the nonlinearity of the photoinduced insulator-to-metal transition. Such nonmonotonous pressure dependence suggests competition between the increase of electronic bandwidth and photoinduced anisotropic lattice strain under pressure.

DOI: 10.1103/PhysRevB.77.125131 PACS number(s): 78.47.-p, 73.20.Mf, 78.55.Kz

I. INTRODUCTION

Ultrafast photoinduced insulator-to-metal (I-M) transitions (PIMTs) have attracted considerable interest for application to switching devices and basic research on nonequilibrium phase dynamics in solids. Actually, PIMTs have been demonstrated in organic and inorganic correlated electron (CE) systems using various ultrafast time-resolved detection methods.[1] On the other hand, application of high pressure is a powerful technique for surveying new material phases in CE systems. The electronic bandwidth competing with the Coulomb repulsion energy can be modulated considerably by applying pressure, engendering superconductivity and the I-M transition.[2,3] By combining the techniques of high pressure and ultrafast spectroscopy,[4] discovery of a new photoinduced phase and a method for control of their dynamics is expected.

Among the many examples of PIMTs,[1] ultrafast and efficient photoinduced PIMTs in 3/4-filled organic salts, which show potential for application to organic devices, have attracted much attention.[5–8] Photoinduced melting of a charge order (CO) in layered [bis(ethylenedithio)]tetrathiafulvalene (BEDT-TTF) (hereinafter ET) salts reflects the contribution of both long-range Coulomb interaction and electron-phonon interaction.[7] That is, microscopic metallic domains on a scale of ~10 nm are generated mainly by an electronic response. For strong excitation, the microscopic domains are condensed to stabilize the semimacroscopic state by accompanying the intermolecular rearrangements. The initially produced microscopic domain is considered to play an important role in PIMT not only in this compound but also in other CE materials.[1] Investigation of pressure effects on PIMTs will elucidate their electronic characteristics as well as the lattice dynamics of the photoinduced microscopic metallic domains. Such knowledge is necessary for exploring new photoinduced states.

This paper reports pressure effects on the PIMT in a typical ET salt α-(ET)$_2$I$_3$ (Ref. 9) using femtosecond pump-probe spectroscopy under hydrostatic pressure. Actually, α-(ET)$_2$I$_3$ exhibits CO at temperatures below T_c (the transition temperature from metal to CO insulator) =135 K.[9–13] The metal-to-CO transition in α-(ET)$_2$I$_3$ is the first-order phase transition, but the lattice effect is not crucial.[14–17] Figure 1(a) shows that T_c decreases with hydrostatic pressure (P [GPa]) (Refs. 18 and 19) because of the increase of the electronic bandwidth, thereby stabilizing the metallic state. We have modulated PIMT dynamics by applying hydrostatic pressure of up to 1 GPa. The electronic nature and the lattice dynamics of the photoinduced microscopic and macroscopic domains were discussed based on the pressure effects on the

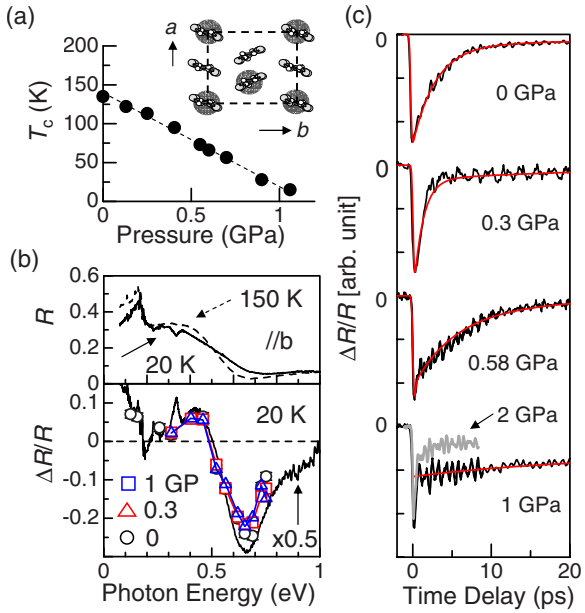

FIG. 1. (Color online) (a) T_c (transition temperature from metal to CO) is plotted as a closed circle; it is a function of pressure (Ref. 18) and the molecular arrangement of α-(ET)$_2$I$_3$. (b) Steady-state (upper panel) and transient (lower panel) reflectivity spectra for $\|b$ at 20 K, t_d=0.1 ps. (c) Time evolutions of $\Delta R/R$ for various P measured at 0.65 eV for I_{ex}=0.1 mJ/cm^2, 20 K. The thick gray curve shows the profile measured at P=2 GPa, 20 K.

lifetime of the photoinduced metallic state and a coherent phonon triggered by the PIMT.

II. EXPERIMENT

Single crystals of α-$(ET)_2I_3$ (average size $1\times1\times0.1$ mm^3) were prepared using a previously reported procedure.[20] Steady-state infrared reflectivity spectra were observed using a microscopic measurement system composed of a microscope (Spectra-Tech IR plan) and a Fourier transform infrared spectrometer (Nicolet Magna 760).[21] For pump-probe spectroscopy, the sample was set in a clamp-type sapphire-anvil cell (Kyowa-Seisakusho K.K. KY04-3) made of BeCu25. Sapphire (1.5 mm diameter culet, 2 mm thickness) was used as an anvil. An inconel gasket with a drilled 0.7 mm diameter hole was used as a sample chamber. The sample was placed in this chamber together with a ruby for calibrating pressure in the pressure medium at 1:1 mixture of Fluorinart 75 and 77. The pressure dependence of T_c, as measured by the change of the reflectivity at 0.65 eV, is analogous to previously reported results,[18,19] confirming that the hydrostatic pressure is applied correctly on the probe spot. A Ti:sapphire amplifier operating at 1 kHz (Hurricane, Spectra-Physics), with a handmade dual optical parametric amplifier (OPA) system, was used as the light source. One OPA, with photon energy (E_{ex}) of 0.89 eV, was used for the pump pulse. The other was used for the probe pulse, ranging from 0.12 to 0.8 eV. Transient reflectivity spectra under hydrostatic pressure were measured at 0.3–0.8 eV. The time resolution of the system was ~200 fs.

III. RESULTS AND DISCUSSIONS

A. Dynamics of photoinduced insulator-to-metal transition in α-$(ET)_2I_3$ under hydrostatic pressure

Figure 1(b) shows polarized reflectivity (R) spectra of α-$(ET)_2I_3$ for the electric field of light parallel to the b axis (upper panel). The R spectra for $T=150$ and 20 K are represented, respectively, as dashed and solid curves. A midinfrared reflection band reflects the I-M transition.[22,23] Open circles, triangles, and rectangles in the lower panel of Fig. 1(b), respectively, show the transient reflectivity ($\Delta R/R$) spectra at 20 K under $P=0$, 0.3, and 1 GPa. The pump and probe lights were polarized parallel to the b axis. These $\Delta R/R$ spectra measured at t_d (the delay time of the probe light after excitation) =0.1 ps are analogous to the differential reflectivity spectra $(R_M-R_I)/R_I$ (solid curves in the lower panel), in which R_M and R_I, respectively, represent the reflectivity of the metallic and the CO insulator phases. This spectral coincidence indicates that melting of the CO and formation of the metallic state occur immediately after photoexcitation, irrespective of P. The magnitude of $\Delta R/R$ observed at any detection energy for $t_d=0.1$ ps increases linearly with the excitation intensity (I_{ex}) up to 0.1 mJ/cm^2, which corresponds to the excitation of approximately one photon per 600 ET molecules.[7] Consequently, the contribution of two-photon absorption is negligible, although large third-order optical nonlinearity has been reported.[24] The PIMT efficiency is evaluated as 250 molecules/photon, indicating that the microscopic metallic domains are initially produced on a ~10 nm scale.

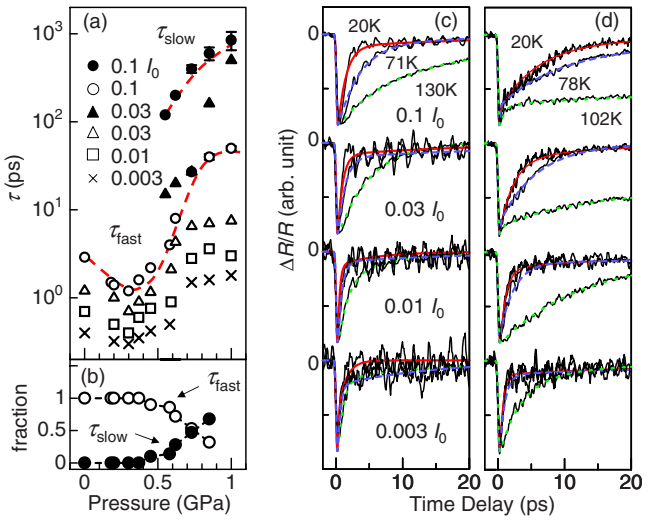

FIG. 2. (Color online) (a) The time constants τ_{fast} and τ_{slow} and (b) their relative fractions as functions of P. In (a), the open circle, triangle, square, and cross, respectively, represent τ_{fast} for $I_{ex}=0.1$, 0.03, 0.01, and 0.003 mJ/cm^2. The closed circle and triangle, respectively, indicate τ_{slow} for $I_{ex}=0.1$ and 0.03 mJ/cm^2. Time evolutions of $\Delta R/R$ for (c) 0.3 GPa and (d) 0.58 GPa at various temperatures and I_{ex}. (I_0 denotes 1 mJ/cm^2). Red, blue, and green curves represent the fitted curves (0.3 GPa [red (gray solid), 20 K; blue (gray dashed), 71 K; green (gray dotted), 130 K], 0.59 GPa [red (gray solid), 20 K; blue (gray dashed), 78 K; green (gray dotted) 102 K]).

Figure 1(c) shows time evolutions of $\Delta R/R$ for various P measured at 0.65 eV ($I_{ex}=0.1$ mJ/cm^2, $T=20$ K). The decay time shortens at 0.3 GPa, but lengthens at 0.58 GPa. The oscillating structures superimposed on the decay curves are attributable to the coherent phonons that are triggered by the instantaneous I-M transition.[7] Details of the coherent phonons are described in Sec. III B. The spikelike ultrafast decay component for $P=1$ and 2 GPa (thick gray curve) is ascribed to the excitation of the semimetallic (SM) state that dominantly exists at pressures greater than 1 GPa.[18,19]

In addition to the coherent phonons and the spikelike component, the decay curves are well characterized by dominant time constants τ_{fast} and τ_{slow} and by their relative fractions, which are plotted, respectively, as open and closed circles as functions of P in Fig. 2(a) [with red (gray) dashed curves] and Fig. 2(b). Here, τ_{fast} and τ_{slow} are evaluated by fitting with a two-component (τ_{fast}, $\tau_{intermediate}$, <0.5 GPa) or a three-component (τ_{fast}, $\tau_{intermediate}$, and τ_{slow}, >0.5 GPa) exponential function [red (gray) curves in Fig. 1(c)]. Among the three components (τ_{fast}, $\tau_{intermediate}$, and τ_{slow}), the small (~5%) intermediate component of $\tau_{intermediate}$ ~15 ps is independent of P and temperature, indicating that it does not involve the PIMT. For $P=0$, these time constants τ_{fast} and τ_{slow} are attributable, respectively, to the microscopic and semimacroscopic metallic domain because τ_{fast} is mainly observed for small I_{ex}, although τ_{slow} becomes dominant for large I_{ex}.[7] As presented in Fig. 2(b), τ_{fast} is a main decay component for $P<0.5$ GPa, but the fraction of τ_{fast} is re-

duced with P. For $P>0.5$ GPa, τ_{slow} in the subnanosecond time scale emerges and becomes dominant, underscoring that generation of the semimacroscopic metallic domain is promoted by the application of pressure. The monotonous increase of τ_{slow} for $P>0.5$ GPa also reflects the stabilization of the semimacroscopic metallic domain. These results for $P>0.5$ GPa are consistent with the decrease in T_c with P [Fig. 1(a)]. In contrast, τ_{fast} shortens for $P<0.5$ GPa and lengthens for $P>0.5$ GPa. Such nonmonotonous change in τ_{fast}, as portrayed in Fig. 2(a), shows that the electronic and/or lattice natures of the photoinduced microscopic domain differ from those of the semimacroscopic metallic domain and the high-temperature (HT) metallic phase. Figures 2(c) and 2(d) show decay curves of $\Delta R/R$ for various I_{ex} and temperatures for $P=0.3$ and 0.58 GPa, respectively. In Fig. 2(a), τ_{fast} and τ_{slow} at 20 K for $I_{ex}=0.003-0.03$ mJ/cm^2 are also depicted. In fact, τ_{slow} is absent for $I_{ex}<0.03$ mJ/cm^2, indicating that the hydrostatic pressure effect on the condensation is efficient for strong excitation, i.e., nonlinearity of the PIMT efficiency measured after several tens of picoseconds becomes prominent by applying pressure.

B. Coherent phonons in the photoinduced insulator-to-metal transition

The oscillating structures in the decay curves are attributable to the coherent phonons triggered by the impulsive change in the electronic state[1,5,7] because they are cosinelike oscillations, i.e., the initial amplitude at $t_d=0$ is not zero.[25] Such a mechanism is analogous to the displacive excitation of the coherent phonons in semiconductors. For that reason, studies of the coherent phonon are useful for clarifying the lattice dynamics in the PIMT. Figures 3(a)–3(c) depict Fourier power spectra for the oscillating components at 0.65 eV for $P=0$, 0.3, and 0.58 GPa, respectively. The upper and lower panels, respectively, show results at $I_{ex}=0.1$ and 0.01 mJ/cm^2. The dashed curve in Fig. 3(a) shows the spectrum for further weak excitation $I_{ex}=0.001$ mJ/cm^2. For $P=0$ GPa, the 48 cm^{-1} mode (arrow 1, orange shade) is prominent at $I_{ex}=0.001$ mJ/cm^2.[7] With increased I_{ex}, the 17 cm^{-1} (arrow 2, red) oscillation increases at I_{ex} of $\sim$0.01 mJ/cm^2, whereas the 29 cm^{-1} band (arrow 3, blue) and the 38 cm^{-1} band (arrow 4, green) become dominant for $I_{ex}=0.1$ mJ/cm^2. Regarding Raman spectra, the corresponding low-frequency modes (45, 38, 30, and $<$20 cm^{-1}) have been reported in α-(ET)$_2$I$_3$ (Refs. 26–29); some are assigned to intermolecular librational modes.[29] It is reasonable to consider that the librational modes support the modulation of the intermolecular transfer integral or equivalently the electronic bandwidth through the change of the dihedral angle and/or the elevation angle between the ET molecules.

Because of the I_{ex} dependence of the Fourier spectrum for $P=0$, the 48 cm^{-1} ($I_{ex}=0.001$ mJ/cm^2) and the 38 cm^{-1} ($I_{ex}=0.1$ mJ/cm^2) oscillations have been attributed, respectively, to the coherent phonons in the CO and metallic states.[7,30] The 29 cm^{-1} oscillation is also considered to be induced in the photoinduced metallic state. However, it remains after relaxation to the CO state, which is possible because the 30 cm^{-1} mode exists in both CO and metallic states, as shown in the Raman spectra.

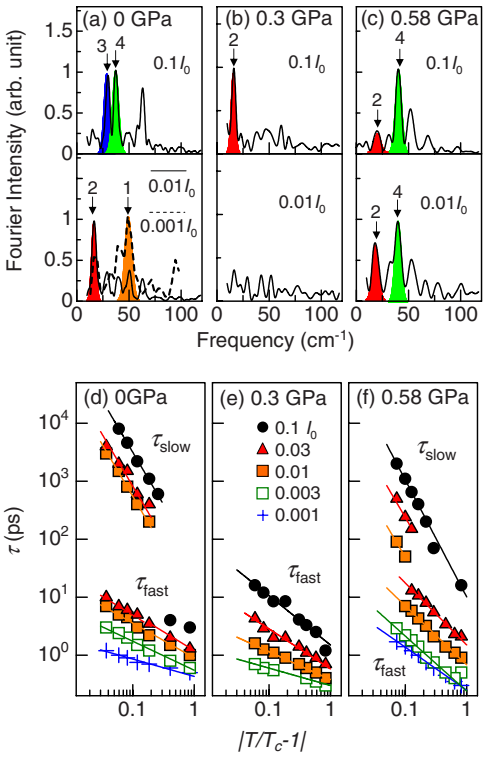

FIG. 3. (Color online) [(a)–(c)] Fourier power spectra for the oscillating component observed for $P=0$, 0.3, and 0.58 GPa, respectively. The dashed curve in (a) shows the Fourier spectrum at $I_{ex}=0.001$ I_0. Arrows 1–4, respectively, indicate the phonon peaks at 48, 17, 29, and 38 cm^{-1}. [(d)–(f)] τ_{fast} and τ_{slow} are plotted, respectively, as functions of reduced temperature $|T/T_c-1|$ for $P=0$, 0.3, and 1 GPa. In the figure, I_0 represents 1 mJ/cm^2.

For $P=0.3$ GPa, as presented in Fig. 3(b), only the 17 cm^{-1} mode is observed to a great degree: the 29 and 38 cm^{-1} modes are suppressed even at strong excitation $I_{ex}=0.1$ mJ/cm^2. The $<$20 cm^{-1} mode in the Raman spectrum is ascribed to the incompletely transformed state of α_t-(ET)$_2$I$_3$, showing superconductivity below 8 K.[29] Observation of the intense 17 cm^{-1} mode for $P=0.3$ GPa suggests that α-(ET)$_2$I$_3$ tends to approach the α_t phase. Considering that α-(ET)$_2$I$_3$ shows superconductivity below 7 K under uniaxial isotropic pressure,[19] a possible interpretation is that photogeneration of the undertransformed α_t phase is promoted by the photoinduced and pressure-induced anisotropic strains for $P=0.3$ GPa. On the other hand, the 38 cm^{-1} mode is dominant, even at weak excitation (0.01 mJ/cm^2) for $P=0.58$ GPa, representing the efficient stabilization of the semimacroscopic metallic domain. With this pressure, the undertransformed α_t phase is considered to be suppressed because the anisotropic effect is overcome by the large hydrostatic pressure and/or the increase of the electronic bandwidth. The relative Fourier intensity of the 38 and 29 cm^{-1} modes I_{38}/I_{29} markedly increases for $>$0.5 GPa, which is attributable to the stabilization of the photoinduced semimacroscopic metallic domain and which is consistent with the interpretation that the 38 cm^{-1} mode is of the photoinduced metallic state.

C. Critical slowing down of the photoinduced metallic state and overall dynamics of photoinduced insulator-to-metal transition under pressure

Another feature of the PIMT in α-$(ET)_2I_3$ is that the relaxation time (τ) of the metallic state shows critical slowing down (CSD),[7] reflecting the reduction of the thermodynamic recovery force of the CO near T_c.[31] The thermodynamic nature of the photoinduced phase transition has been extracted from the CSD.[32,33] Figures 3(d), 3(e), and 3(f), respectively, depict τ_{fast} and τ_{slow}, which are plotted as functions of reduced temperature $|T/T_c-1|$ for $P=0$, 0.3, and 0.58 GPa. Actually, τ_{slow} for $I_{\mathrm{ex}}=0.01-0.1$ mJ/cm^2 increases near T_c and is represented as $\tau_{slow} \propto |T/T_C-1|^{-1.8}$, whose exponent (1.8) shows that νz (ν and z are critical exponents of the correlation length ξ and the dynamic critical exponent, respectively). The value of νz is nearly equal to the calculated value (2.1665), as evaluated by Monte Carlo simulation within the framework of the two-dimensional Ising model.[34] Because macroscopic fluctuation is assumed for the calculation, that similarity of the exponent νz shows that τ_{slow} is ascribed to the relaxation of the macroscopic metallic domain. On the other hand, the weaker dependence of τ_{fast}, whose exponent is evaluated as $0.3(0.001\ \mathrm{mJ/cm^2})-0.6(0.03\ \mathrm{mJ/cm^2})$, reflects that the thermodynamic nature of microscopic domains differs from that of the macroscopic metallic state.[7] For $P=0.3$ GPa [Fig. 3(e)], τ_{slow} showing $\tau_{slow} \propto |T/T_C-1|^{-1.8}$ was not detected even for large I_{ex} (=0.1 mJ/cm^2). The absence of τ_{slow} for $P=0.3$ GPa indicates that the condensation of the metallic domains is disturbed. For $P=0.58$ GPa, the exponent of τ_{slow} is 2.1, confirming that τ_{slow} is attributable to the semimacroscopic metallic domain, which is analogous to that for $P=0$.

The SM state should also be considered as an origin of τ_{slow} for $P=0.58$ GPa because such a state is another quasistable state under pressure.[18,19] However, observations of the critical exponent $\nu z \sim 2$ and the 38 cm^{-1} coherent phonon for $P=0.58$ GPa show no marked difference from those for $P=0$. Consequently, the generation of a metallic state that is analogous to that for $P=0$ is suggested.

Considering the observation of the coherent intermolecular librational phonons, we propose the schematic potential model portrayed in Fig. 4. It is difficult to interpret the characteristic molecular rearrangements in the I-M transition because the structural change is small.[14–17] The structural change in the I-M transition of this compound remains controversial. Nevertheless, observations of low-frequency coherent phonons enable us to speculate that the PIMT is accompanied by intermolecular librational displacements, as illustrated by Fig. 4.

For $P=0$, the initially produced microscopic metallic domain is condensed to the semimacroscopic metallic domain, as presented in Fig. 4(a). For $P<0.5$ GPa, the photoinduced anisotropic strain of the microscopic metallic domain promotes instability toward the α_t phase [Fig. 4(b)]. At higher pressure ($P>0.5$ GPa), however, the instability is considered to be overcome by a further increase in the bandwidth or isotropic strain by the hydrostatic pressure, thereby stabilizing the metallic domain in the original α phase, as shown in Fig. 4(c).

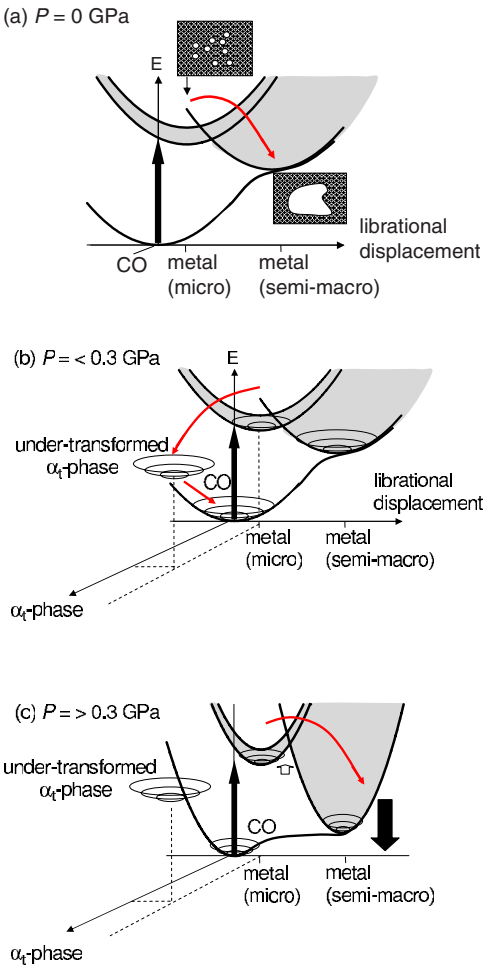

FIG. 4. (Color online) Schematic illustration of the adiabatic potential energy surfaces of CO, photoinduced microscopic metallic domain, and semimacroscopic metallic domain. (a) $P=0$ GPa, (b) $P<0.5$ GPa, and (c) $P>0.5$ GPa.

IV. SUMMARY

In summary, high-pressure effects on the photoinduced I-M transition were demonstrated in α-$(ET)_2I_3$ using femtosecond spectroscopy under hydrostatic pressure. Marked changes of the lifetime of the photoinduced metallic state and the coherent phonon depending on the pressure P revealed that the condensation of the photoinduced microscopic metallic domain to the semimacroscopic domain is disturbed for $P<0.5$ GPa. On the other hand, for $P=0.5-1$ GPa, condensation is promoted. Such nonmonotonous pressure dependence indicates that the electronic and lattice natures of the microscopic metallic domain differ from those of the macroscopic metal. Condensation of the microscopic domain is suggested to compete with the generation of undertransformed α_t-$(ET)_2I_3$ phase, which indicates superconductivity below 8 K.

ACKNOWLEDGMENTS

We thank K. Yonemitsu, K. Iwano, S. Ishihara, H. Matsueda, A. Takahashi, H. Sawa, M. Watanabe, and Y. Nishio for their helpful discussions. This work was partially supported by Grants-in-Aid for Scientific Research from the Ministry of Education, Culture, Sports, Science, and Technology and from the Casio Science Promotion Foundation.

*s.iwai@sspp.phys.tohoku.ac.jp

[1] Special issue on photoinduced phase transition and their dynamics, edited by M. Kuwata-Gonokami and S. Koshihara, J. Phys. Soc. Jpn. **75**, 011001 (2006).
[2] M. Imada, A. Fujimori, and Y. Tokura, Rev. Mod. Phys. **70**, 1039 (1998).
[3] K. Murata, S. Kagoshima, S. Yasuzuka, H. Yoshino, and R. Kondo, J. Phys. Soc. Jpn. **75**, 051015 (2006).
[4] M. Kasami, T. Mishina, and J. Nakahara, Phys. Status Solidi B **241**, 3113 (2004).
[5] M. Chollet, L. Guerin, N. Uchida, S. Fukaya, H. Shimoda, T. Ishikawa, K. Matsuda, T. Hasegawa, A. Ohta, H. Yamochi, G. Saito, R. Tazaki, S. Adachi, and S. Koshihara, Science **307**, 86 (2005).
[6] N. Tajima, J. Fujisawa, N. Naka, T. Ishihara, R. Kato, Y. Nishio, and K. Kajita, J. Phys. Soc. Jpn. **74**, 511 (2005).
[7] S. Iwai, K. Yamamoto, A. Kashiwazaki, F. Hiramatsu, H. Nakaya, Y. Kawakami, K. Yakushi, H. Okamoto, H. Mori, and Y. Nishio, Phys. Rev. Lett. **98**, 097402 (2007).
[8] K. Yamamoto, S. Iwai, S. Boyko, A. Kashiwazaki, F. Hiramatsu, C. Okabe, N. Nishi, and K. Yakushi (unpublished).
[9] K. Bender, I. Henning, D. Schweitzer, K. Dietz, H. Endre, and H. J. Keller, Mol. Cryst. Liq. Cryst. **108**, 359 (1984).
[10] J. Moldenhauer, Ch. Horn, K. I. Pokhodnia, and D. Schweitzer, Synth. Met. **60**, 31 (1993).
[11] H. Kino and H. Fukuyama, J. Phys. Soc. Jpn. **65**, 2158 (1996).
[12] Y. Takano, K. Hiraki, H. M. Yamamoto, T. Nakamura, and T. Takahashi, Synth. Met. **120**, 1081 (2001).
[13] R. Wojciechowski, K. Yamamoto, K. Yakushi, M. Inokuchi, and A. Kawamoto, Phys. Rev. B **67**, 224105 (2003).
[14] Y. Tanaka and K. Yonemitsu, J. Phys. Soc. Jpn. **77**, 034708 (2008).
[15] H. Endres, H. J. Keller, R. Swietlik, D. Schweitzer, K. Angermund, and Kruger, Z. Naturforsch. Teil A **41A**, 1319 (1986).
[16] T. J. Emge, P. C. W. Leung, M. A. Beno, H. H. Wang, and J. M. Williams, Mol. Cryst. Liq. Cryst. **138**, 393 (1986).
[17] T. Kakiuchi, Y. Wakabayashi, H. Sawa, T. Takahashi, and T. Nakamura, J. Phys. Soc. Jpn. **76**, 113702 (2007).
[18] H. Schwenk, P. Gross, C. P. Heidmann, K. Andres, D. Schweitzer, and H. Keller, Mol. Cryst. Liq. Cryst. **119**, 329 (1985).
[19] N. Tajima, A. Ebina-Tajima, M. Tamura, Y. Nishio, and K. Kajita, J. Phys. Soc. Jpn. **71**, 1832 (2002).
[20] H. Anzai, M. Tokumoto, T. Ishiguro, G. Saito, H. Kobayashi, R. Kato, and A. Kobayashi, Synth. Met. **19**, 611 (1987).
[21] K. Yamamoto, K. Yakushi, K. Miyagawa, K. Kanoda, and A. Kawamoto, Phys. Rev. B **65**, 085110 (2002).
[22] K. Yakushi, H. Kanbara, H. Tajima, H. Kuroda, G. Saito, and T. Mori, Bull. Chem. Soc. Jpn. **60**, 4251 (1987).
[23] M. Dressel, G. Gruner, J. P. Pouget, A. Breining, and D. Schweitzer, J. Phys. I **4**, 579 (1994).
[24] P. G. Huggard, W. Blau, and D. Schweitzer, Appl. Phys. Lett. **51**, 2183 (1987).
[25] H. Zeiger, J. Vidal, T. K. Cheng, E. P. Ippen, G. Dresselhaus, and M. S. Dresselhaus, Phys. Rev. B **45**, 768 (1992).
[26] R. Swietlik, D. Schweitzer, and H. J. Keller, Phys. Rev. B **36**, 6881 (1987).
[27] J. Moldenhauer, U. Niebling, T. Ludbig, B. Thoma, D. Schweitzer, W. Strunz, H. J. Keller, P. Bele, and H. Brunner, Mol. Cryst. Liq. Cryst. Sci. Technol., Sect. A **284**, 161 (1996).
[28] T. Ludwig, D. Schweitzer, and H. J. Keller, Solid State Commun. **96**, 961 (1995).
[29] K. I. Pokhodina, A. Graja, M. Weger, and D. Schweitzer, Z. Phys. B: Condens. Matter **90**, 127 (1993).
[30] The 38 cm^{-1} mode is also observed for the HT metallic state through the impulsive stimulated Raman scattering process (Ref. 7). This supports our assignment of the 38 cm^{-1} mode. However, the 38 cm^{-1} mode has been assigned to the intermolecular mode of the CO state from the Raman study in the powder of ET (Ref. 27). This disagreement might be attributable to the experimental condition of the Raman measurement of the powder sample (nonpolarized excitation at 466 or 674 nm, near the I_3^- absorption) differing from those of our measurement ($\|b$ polarized excitation at 1400 nm, near the CT absorption).
[31] P. C. Hohenberg and B. I. Hailerin, Rev. Mod. Phys. **49**, 435 (1977).
[32] X. J. Liu, Y. Moritomo, A. Nakamura, H. Tanaka, and T. Kawai, Phys. Rev. B **64**, 100401(R) (2001).
[33] T. Kise, T. Ogasawara, M. Ashida, Y. Tomioka, Y. Tokura, and M. Kuwata-Gonokami, Phys. Rev. Lett. **85**, 1986 (2000).
[34] M. P. Nightingale and H. W. J. Blote, Phys. Rev. Lett. **76**, 4548 (1996).